Biochemical Pharmacology 80 (2010) 1427–1436

Contents lists available at ScienceDirect

Biochemical Pharmacology

journal homepage: www.elsevier.com/locate/biochempharm

Y124 at the peripheral anionic site is important for the reactivation of nerve agent-inhibited acetylcholinesterase by H oximes

Chunyuan Luo [*], Carolyn Chambers [2], Nagarajan Pattabiraman [1], Min Tong [1], Prasanthi Tipparaju [1], Ashima Saxena [1]

Division of Bacterial and Rickettsial Diseases, Walter Reed Army Institute of Research, Silver Spring, MD 20910-7500, USA

ARTICLE INFO

Article history:
Received 14 May 2010
Accepted 13 July 2010

Keywords:
Bovine acetylcholinesterase
Cyclosarin
VR
Oxime reactivation
Peripheral anionic site
Molecular modeling

ABSTRACT

The toxicity of organophosphorus (OP) nerve agents is manifested through irreversible inhibition of acetylcholinesterase (AChE) at the cholinergic synapses, which stops nerve signal transmission, resulting in a cholinergic crisis and eventually death of the poisoned person. Oxime compounds used in nerve agent antidote regimen reactivate nerve agent-inhibited AChE and halt the development of this cholinergic crisis. Due to diversity in structures of OP nerve agents, none of the currently available oximes is able to reactivate AChE inhibited by different nerve agents. To understand the mechanism for the differential activities of oximes toward AChE inhibited by diverse nerve agents in order to aid the design of new broad-spectrum AChE reactivators, we undertook site-directed mutagenesis and molecular modeling studies. Recombinant wild-type and mutant bovine (Bo) AChEs were inhibited by two bulky side-chain nerve agents, GF and VR, and used for conducting reactivation kinetics with five oximes. A homology model for wild-type Bo AChE was built using the recently published crystal structure of human AChE and used to generate models of 2-PAM and HI-6 bound to the active-sites of GF- and VR-inhibited Bo AChEs before nucleophilic attack. Results revealed that the peripheral anionic site (PAS) of AChE as a whole plays a critical role in the reactivation of nerve agent-inhibited AChE by all 4 bis-pyridinium oximes examined, but not by the mono-pyridinium oxime 2-PAM. Of all the residues at the PAS, Y124 appears to be critical for the enhanced reactivation potency of H oximes.

Published by Elsevier Inc.

1. Introduction

Organophosphorus (OP) chemical warfare agents, such as tabun (GA), sarin (GB), soman (GD), cyclosarin (GF), VR and VX, pose significant threats to both military and civilian populations due to their possible use in battlefield and terrorist acts. The acute toxicity of OP nerve agents is generally attributed to the irreversible inhibition of synaptic acetylcholinesterase (AChE; EC 3.1.1.7), an enzyme responsible for hydrolyzing the neurotransmitter acetylcholine (ACh) at the pre-synapses and terminating signal transmission at the cholinergic synapses. The accumulation of ACh causes over-stimulation of post-synaptic receptors, which results in a variety of cholinergic effects, including miosis, increased tracheobronchial and salivary secretions, muscle fasciculations and seizures, and respiratory failure [1]. Although the current antidotal regimen against nerve agent poisoning contains different components such as an anticholinergic atropine, an anticonvulsant diazepam, and an oxime reactivator such as 2-PAM or obidoxime, oxime is the main determinant of the therapeutic efficacy since it is responsible for reversing the key step in poisoning—the recovery of nerve agent-inhibited AChE. However, both experimental data and clinical findings have demonstrated that different oximes are not equally effective against poisonings caused by structurally different OP compounds. For example, the efficacy of mono-pyridinium oxime 2-PAM is very limited against poisoning by GD and GF [2,3]. For this reason, numerous studies over the last several decades have focused on developing oximes with enhanced reactivation efficiency. More potent bis-pyridinium oximes such as trimedoxime bromide (TMB4) and obidoxime were examined and obidoxime was fielded by most European countries [4]. Although these bis-pyridinium oximes demonstrated improved efficacy against poisoning by most nerve agents, the improvement was very little against certain nerve agents such as soman and GF.

* Corresponding author. Present address: Division of Bacterial & Rickettsial Diseases, Walter Reed Army Institute of Research, 503 Robert Grant Ave, Silver Spring, MD 20910, USA. Tel.: +1 310 319 9089; fax: +1 301 319 9801.
E-mail address: chunyuan.luo@us.army.mil (C. Luo).
[1] Present address: Division of Bacterial & Rickettsial Diseases, Walter Reed Army Institute of Research, Silver Spring, MD 20910, USA.
[2] Present address: Research Division, Physiology & Immunology Branch, US Army Medical Research Institute of Chemical Defense, Aberdeen Proving Ground, MD 21010-5400, USA.

0006-2952/$ – see front matter. Published by Elsevier Inc.
doi:10.1016/j.bcp.2010.07.020

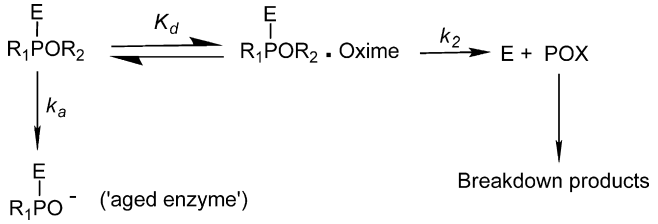

Fig. 1. Two-step reaction for the oxime reactivation of OP-inhibited AChE by oxime.

Therefore, in the 70s and 80s, new promising bis-pyridinium oximes, the so-called Hagerdorn oximes (H oximes) HI-6 and HLo-7 were synthesized and shown to be very powerful reactivators of GD-inhibited AChE [5,6]. While HI-6 is ineffective in reactivating GA-inhibited AChE [7,8], HLo-7 is able to slowly reactivate GA-inhibited AChE [9]. However, due to the poor stability of HLo-7 in aqueous solutions and difficulty in synthesis, it is not suitable for use as a nerve agent antidote [10]. Despite decades of research, none of the oximes is a broad-spectrum reactivator which can cover all potential threat agents. Therefore, the development of the next generation of broad-spectrum oximes faces significant challenges. To take this challenge and create tools for developing more potent and broad-spectrum oximes, a better understanding of the oxime reactivation mechanism of nerve agent-inhibited AChE is warranted.

During the past decade, numerous studies have investigated the mechanism of oxime reactivation of OP-inhibited AChE [11–14]. The active-site of human AChE constitutes three amino acid residues, S203, E334, and H447 buried close to the bottom of a deep and narrow gorge lined with 14 conserved aromatic amino acid residues [15]. The catalytic anionic binding site (CAS) residues including W86 and Y337 facilitate the orientation and binding of the positively charged substrate ACh. Another important site is the peripheral anionic site (PAS), which constitutes Y72, Y124, and W286, and an anionic residue D74. The function of the PAS may be for trapping the substrate down to the narrow active gorge [16], or for allosteric modulation of enzyme during catalysis [17]. The inhibition of AChE by an OP nerve agent involves the formation of a covalent bond between the γ-oxygen of the active-site S203 with the phosphorus atom of the OP compound. The reactivation of OP-inhibited AChE proceeds via a two-step reaction (Fig. 1). The first step is to form a fully reversible Michaelis-type phosphoryl-AChE complex (penta-coordinate transition state). The second step is the displacement of the phosphoryl residue from the transition state by forming an intermediate called phosphoryl oxime (POX) [18]. K_d is the dissociation constant, which is inversely proportional to the affinity of the oxime to the phosphoryl AChE. The reactivity of the oxime can be expressed by the rate constant k_2, describing the specific reactivity. The figure also shows the competing 'aging' reaction, in which the AChE–OP conjugate is converted into a negatively charged 'aged' conjugate, which cannot be reactivated by current reactivators; k_a is the 'aging' rate constant for this reaction.

Since reactivation is an enzyme-facilitated nucleophilic reaction, both nucleophilicity and orientation of the nucleophile in the active center with respect to the OP structure are important factors that influence the effectiveness of the oxime. Another important factor governing the reactivatibility of OP-inhibited AChE is 'aging', which is a process of dealkylation (leaving of one of the alkyl groups from the AChE–OP conjugate). Once dealkylation occurs, the enzyme can no longer be reactivated by any known oxime. This is especially significant for GD-inhibited AChE, since the 'aging' of this conjugate is very rapid with an aging half-time of <1–30 min depending on the source of enzyme [19,20]. The difficulty in reactivating GD-inhibited AChE was once believed to be solely due to the 'aging' of the inhibited enzyme. However, HI-6 and HLo-7, were shown to be able to rapidly reactivate GD-inhibited AChE prior to 'aging' as compared to other bis-pyridinium oximes [6,8]. Therefore, steric hindrance from the bulky pinacolyl group of GD is also thought to be a significant factor for the slow reactivation of GD-inhibited AChE. Indeed, the reactivation of AChE inhibited with GF, also a nerve agent containing a bulky cyclohexyl side-chain, by 2-PAM was found to be similarly slow although the 'aging' of GF-inhibited AChE is much slower than GD-inhibited enzyme [21–23]. Studies with another relatively bulky side-chain nerve agent, VR, also showed a similar phenomenon, though to a lesser degree because the 4-carbon iso-butyl side-chain of VR is smaller than the 6-carbon side-chains of GD and GF [3,24–26]. But, studies with recombinant human AChE suggested that H oximes can overcome the steric hindrance imposed by these bulky side-chains and reactivate GD-, GF-, and VR-inhibited AChE at rates that are 27–110-fold faster than those for AChE inhibited by GB and VX [24].

Previous studies have suggested that bis-pyridinium oximes may use residues at the PAS to orient nucleophilic attack by oxime. A study with MEPQ-inhibited mouse triple mutant (Y72N/Y124Q/W286A) AChE suggested this possibility since this mutant had a significantly reduced reactivation by the bis-pyridinium oxime HI-6 but not by the mono-pyridinium oxime 2-PAM [26]. The interaction between the second-pyridinium structure and different PAS residues of AChE is also supported by modeling and X-ray crystallographic studies [13,27–29]. In order to understand the role of different PAS residues in oxime reactivation of nerve agent-inhibited AChE, we cloned and expressed wild-type and different site-specific mutant bovine (Bo) AChEs in Chinese Hamster Ovary (CHO) cells. The enzymes were purified and inhibited with nerve agents GF and VR, for conducting reactivation kinetics by one mono-pyridinium and four bis-pyridinium oximes. Also, homology modeling and docking were used to simulate the binding of oximes to GF- and VR-inhibited Bo AChEs. Due to a 95% homology between human and Bo AChE sequences, a homology model for wild-type Bo AChE was built using the recently published crystal structure of human apo-AChE (PDB ID:3LII, http://www.rcsb.org). This homology model was used to generate models of 2-PAM and HI-6 bound to the active-sites of GF- and VR-inhibited Bo AChEs before nucleophilic attack. Results support those from reactivation kinetic studies and highlight the importance of PAS residues as a whole for enhancing the reactivation of OP-inhibited AChE by bis-pyridinium oximes, and Y124 for specific oximes such as HI-6 and HLo-7.

2. Materials and methods

2.1. Reagents, oximes, and nerve agents used in the study

Acetylthiocholine iodide (ATC) and 5,5-dithiobis-(2-nitrobenzoic acid) (DTNB) were from Sigma Chemical Co. (St. Louis, MO) and Bio-Spin 6 chromatography columns were from Bio-Rad (Hercules, CA). Oximes 2-PAM, HI-6, HLo-7, MMB-4, and ICD-585 (Fig. 2A) were obtained from the Division of Experimental Therapeutics, Walter Reed Army Institute of Research. The purity of all oximes was >99% as determined by elemental and HPLC analyses. Enzyme conjugates with nerve agents GF and VR (Fig. 2B) obtained from the U.S. Army Edgewood Chemical and Biological Center (Aberdeen Proving Ground, MD) were prepared at the U.S. Army Medical Research Institute of Chemical Defense (Aberdeen Proving Ground, MD). The purity of all nerve agents was >98.5% as determined by ^{31}P NMR.

2.2. Cloning and expression of recombinant wild-type and mutant Bo AChEs

2.2.1. Cloning of Bo AChE cDNA

Total RNA was isolated from calf brain using RNAzol B (Tel-Test, Inc., Friendswood, TX) according to the manufacturer's specifica-

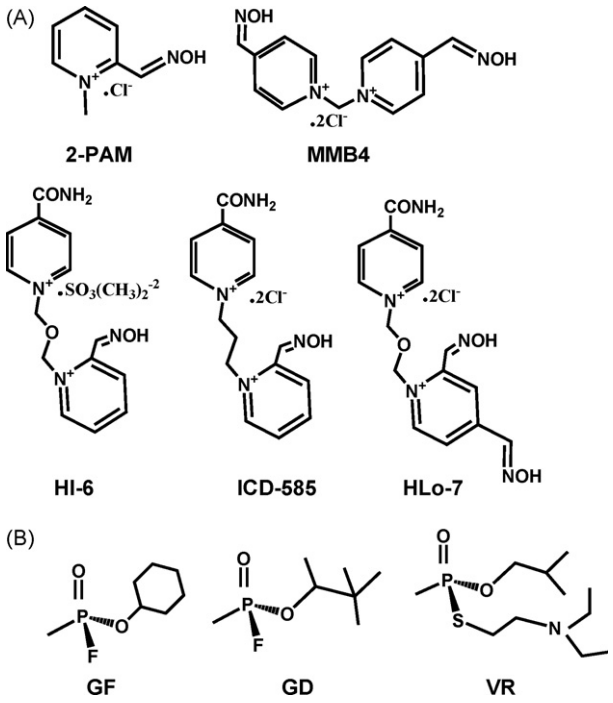

Fig. 2. (A) Structures of oximes used for the reactivation of nerve agent-inhibited recombinant wild-type and mutant Bo AChEs; (B) structures of organophosphorus nerve agents.

tions. The coding sequence for the Bo AChE was obtained using RT-PCR amplification of the total RNA as specified by Applied Biosystems (Foster City, CA). Many PCR fragments were isolated and subcloned into TA vector pCR2.1 (Invitrogen, Carlsbad, CA) using the manufacturer's specifications. Two clones were chosen for further cloning efforts: one (which contained all of exon 2 minus the signal peptide sequence) and two (which contained approximately 70 base pairs of exon 2 sequence, but all of the sequences for exons 3, 4, and 6). Each clone was digested with restriction enzymes EcoRI and NcoI, and subcloned as a single restriction fragment into the EcoRI site of the pGEM7Z vector. Colonies were screened for the proper orientation and insert size. A clone was obtained which contained the entire full length Bo AChE cDNA sequence in the correct orientation with the correct size in base pairs. Both strands of this clone were sequenced to determine its correctness. The sequence was compared (using BLAST) with the known Bo AChE sequences in GenBank database under accession numbers AF061813, AF061814, AF061815, and AF061816 representing exons 2, 3, 4, and 6, respectively.

2.2.2. Cloning Bo AChE cDNA into pCIneo mammalian expression vector

The signal peptide sequence of Bo AChE was determined through PCR amplification of bovine genomic kidney DNA using degenerate oligonucleotides to the bovine signal peptide amino acid sequence and an oligonucleotide made from the coding sequence found at the end of exon 2 utilizing the high fidelity Pfx DNA polymerase from Invitrogen (Carlsbad, CA). Both strands of this PCR fragment were sequenced to determine its correctness. An EcoRI site was placed at the 5′ end of the PCR fragment and an NcoI site was found near the end of exon 2. The PCR generated genomic DNA fragment (containing exon 2 and the bovine signal peptide sequence), and the Bo AChE cDNA (containing exons 3, 4, and 6) from the pGEM7Z clone were digested with the restriction enzymes (EcoRI and NcoI), fragmented by agarose gel electrophoresis, the desired DNA fragments were isolated, agarose gel DNA purified, and ligated together. Therefore, a continuous open reading frame coding for the Bo AChE T-subunit was subcloned into the EcoRI site of the pCIneo vector from Promega.

2.2.3. Establishment of stable cell lines expressing Bo AChEs

The establishment of stable cell lines expressing Bo AChEs was conducted similarly as that described previously for the expression of rhesus monkey AChE [30].

2.2.4. Mutagenesis of recombinant Bo AChE

Site-directed mutagenesis was conducted using the Quik-Change II XL Site-Directed Mutagenesis Kit protocols (Stratagene, La Jolla, CA). PCR was performed using pairs of forward and reverse mutagenic oligonucleotide primers. The desired mutation occurred at the same position but on opposite strands of the plasmid. After site-directed mutagenesis was completed, colonies were picked, grown as minipreps, and their DNAs were isolated and sequenced to identify the mutation and to confirm that no spurious changes had occurred. In the case of the quadruple mutant Y72N/D74G/Y124Q/W286A, it was necessary to make each change separately before proceeding to the next mutation. Each mutant DNA clone was used to perform transfection of CHO-K1 cells, transient expression, and establishment of a stable cell line as described above.

2.2.5. Purification of recombinant Bo AChEs

Recombinant wild-type and mutant Bo AChEs expressed in the cell media of CHO cells were purified using procainamide-sepharose 4B gel (Sigma Chemical Co., MO) [31] followed by anion exchange chromatography using DEAE Sepharose Fast Flow gel (Pharmacia, NJ) in 50 mM sodium phosphate buffer, pH 8.0. The (Y72N/D74G/Y124Q/W286A) quadruple mutant AChE did not bind to procainamide-sepharose 4B gel and the tetrameric form of this enzyme was partially purified by gel filtration chromatography on a 1.5 M Bio Gel A column (Bio-Rad, CA).

2.3. Enzyme kinetic studies

2.3.1. Assay for AChE activity

AChE activity was determined by the Ellman method [32]. The assay mixture contained 1 mM ATC as the substrate and 0.5 mM DTNB in 50 mM sodium phosphate buffer, pH 8.0. The formation of product was measured at 412 nm at 25 °C.

2.3.2. Determination of rate constants for the reactivation of nerve agent-inhibited AChEs by oximes

Kinetic constants for the reactivation of nerve agent-inhibited AChEs were determined using a non-continuous method used [13]. However, in order to minimize the aging of nerve agent-inhibited AChEs, enzyme conjugates for reactivation studies were prepared in 100 mM TAPS buffer, pH 9.5. Excess nerve agent was either removed from AChE–nerve agent conjugate by passing the solution through a Bio-Spin 6 column or neutralized by adding fresh enzyme to the solution. AChE–nerve agent conjugates were stored at −20 °C in 50% glycerol until use. Oxime reactivation was initiated by making at least a 20-fold dilution of the AChE–nerve agent conjugate in 50 mM sodium phosphate buffer, pH 8.0, containing 0.05% bovine serum albumin (BSA) and different concentrations of oxime. The solution was maintained at 25 °C and at specified time intervals, 5–10 μl of the reactivation mixture was transferred into a cuvette containing 1–3 ml of assay mixture, to monitor AChE activity. The final concentration of enzyme in the assay mixture varied from 0.01 to 0.1 nM. Three control groups (AChE control, nerve agent-inhibited AChE control and AChE with oxime control) were also set up for the simultaneous monitoring of AChE activity at different time intervals. Four to six oxime concentrations ranging from 1 μM to 6.4 mM were used for

determining the reactivation rate constants depending on the oxime and OP conjugate. In order to minimize the possible re-inhibition of reactivated enzyme by POX and to ensure an accurate determination of the reactivation rate constants, the concentration of AChE–nerve agent conjugate was kept as low as possible, and 0.05 U/ml of rabbit paraoxonase (PON1) was included in the reactivation media to break down any POX formed during reactivation process [33,34]. PON1 from rabbit serum was purified following a previously reported procedure using column chromatography of Cibacron Blue 3GA-agarose Type 3000CL gel (Sigma, MO) and DEAE Sepharose Fast Flow gel (Pharmacia, NJ) [35]. The first-order reactivation rate constant, k_{obs}, was determined by fitting the experimental data to the equation for one-phase exponential association:

$$\%\,(E_{react})_t = A(1 - e^{-k_{obs}\cdot t}) \quad (1)$$

where t is the time at which the sample was withdrawn; $\%\,(E_{react})_t$ is percent reactivation measured at time t; and A is percent of maximum reactivation measured after 24 h.

A secondary plot of k_{obs} vs. [oxime] was used to obtain the overall reactivation rate constant:

$$k_{obs} = \frac{k_2}{1 + K_{ox}/[\text{oxime}]} \quad (2)$$

$$k_r = \frac{k_2}{K_{ox}} \quad (3)$$

where k_2 is the intrinsic reaction constant; K_{ox} is the apparent equilibrium constant; and k_r is the overall reactivation rate constant.

2.4. Molecular modeling studies

The three-dimensional coordinates for the model of Bo AChE were generated using the published sequence of Bo AChE [36] and the crystal structure of human apo-AChE (PDB ID:3LII; http://www.rcsb.org) as the template. The homology model of Bo AChE was built using only the protein chain (A-chain) of human apo-AChE and the homology building module of MOE (Molecular Operating Environment, Chemical Computing Group, Quebec, Canada). The initial homology model was subjected to energy minimization using MMF94x force field available in MOE. The homology model was further refined using the protein contact and protein geometry modules of MOE. The energy minimized model of Bo AChE was further refined by subjecting it to a molecular dynamics (MD) equilibration of 50 ps, a MD simulation of 200 ps, followed by energy minimization. For all the above calculations, the reaction field salvation model was considered to mimic solvent molecules. Energy minimized models for Bo AChE inhibited by the *S*-isomers of GF or VR, were generated by covalently linking the OPs to γ-oxygen of the active-site S203 in Bo AChE followed by energy minimization using the above protocol.

To simulate the position and the orientation of an oxime before reactivation, the mono-pyridinium oxime, 2-PAM was manually docked into the active-site of GF-inhibited Bo AChE, such that the distance between the nucleophile oxygen of 2-PAM and the phosphorus atom of GF covalently attached to the γ-oxygen of the active-site S203 was restrained around 4.2 Å and the angle formed by the γ-oxygen of the active-site S203, the phosphorus atom of GF and the nucleophile oxygen of 2-PAM was restrained around 160°. The distance and angle restrains were required for 2-PAM to position and orient for a productive nucleophilic attack. This minimized structure was subjected to a short MD simulation using MOE in order to better fit the oxime into the binding site. The above mentioned constraints for the distance (~4.2 Å) and the angle (~160°) were placed during all MD simulation. At the end of the MD simulation, the model of the GF-inhibited Bo AChE·2-PAM complex was subjected to energy minimization in order to generate the final model of the complex. The above procedure was repeated to generate the final energy minimized model for VR-inhibited Bo AChE·2-PAM complex.

The three-dimensional model for HI-6 was generated by calculating the energies of various conformations of HI-6 produced by varying all single bonds using MOE. From the conformation energy values, one hundred forty seven energetically favorable unique conformations for HI-6 were identified. The ring containing the attacking oxime group of HI-6 was superposed on the corresponding structure of 2-PAM in the energy minimized structure of GF-inhibited Bo AChE·2-PAM complex. Because there are two ways of superposing the two six-membered aromatic rings between 2-PAM and HI-6, many orientations of HI-6 in the active-site gorge of Bo AChE were generated. From the calculated interaction energies of HI-6 with GF-inhibited Bo AChE, the complex with the highest favorable interaction energy was identified. As discussed above for the docking of 2-PAM, energy minimization followed by MD simulations were carried out in order to generate the final energy minimized models for GF-inhibited Bo AChE·HI-6 complex. The same procedure was used for generating the final energy minimized model for VR-inhibited Bo AChE·HI-6 complex.

3. Results

Five different oximes (Fig. 2A) were examined in our reactivation kinetic studies with the recombinant wild-type and six single and one quadruple mutant Bo AChEs after inhibition with nerve agents GF and VR. The reason for choosing GF and VR for these studies was that these two nerve agents are similar to GD in that they contain bulky side-chain structures, which may significantly hinder reactivation by oximes [3,13,24,25]. Due to the rapid aging of GD-inhibited AChE, we did not conduct studies with this conjugate. Fig. 3 shows the reactivation kinetic profile of GF-inhibited wild-type Bo AChE by MMB4. In this and similar cases, the plot of pseudo first-order reactivation rate constant (k_{obs}) vs. [oxime] yielded a saturation curve, and the overall reactivation rate constant (k_r) was obtained by dividing the intrinsic reaction constant k_2 by dissociation constant K_{ox}. However in some cases the plot of k_{obs} vs. [oxime] was linear as shown for the reactivation of VR-inhibited Y72N Bo AChE by HLo-7 (Fig. 4). Under such situations, K_{ox} and k_2 could not be determined and k_r was estimated from the slope of the line. The estimation of the k_r value using the slope of the linear line for the second-order oxime reactivation constant has been used in many previous studies [24,26]. Under such situations, the active-sites of the enzyme conjugate have not been fully occupied by oxime with the oxime concentration that still allows the measurement of reactivation progress, making linear regression for k_r approximation reasonable.

Tables 1–3 summarize different rate constants (k_2, K_{ox}, and k_r) for the reactivation of GF-inhibited recombinant wild-type and mutant Bo AChEs with five oximes. The reactivation potency of these oximes measured by k_r values follows the rank order: HLo-7 > HI-6 > ICD-585 > MMB4 > 2-PAM. From the K_{ox} and k_2 values, it is obvious that both parameters contribute to the higher reactivation rate (k_r) of the 4 bis-pyridinium oximes compared with the mono-pyridinium oxime 2-PAM, but a lower K_{ox} value contributes to a higher k_r. Of different mutant Bo AChEs examined, mutations of D74 to Gly and Y337 to Ala resulted in significantly faster oxime reactivations compared to wild-type enzyme in most cases. The other four single PAS mutants (Y72N, Y124Q, Y124F, and W286A) all showed reduced reactivations to

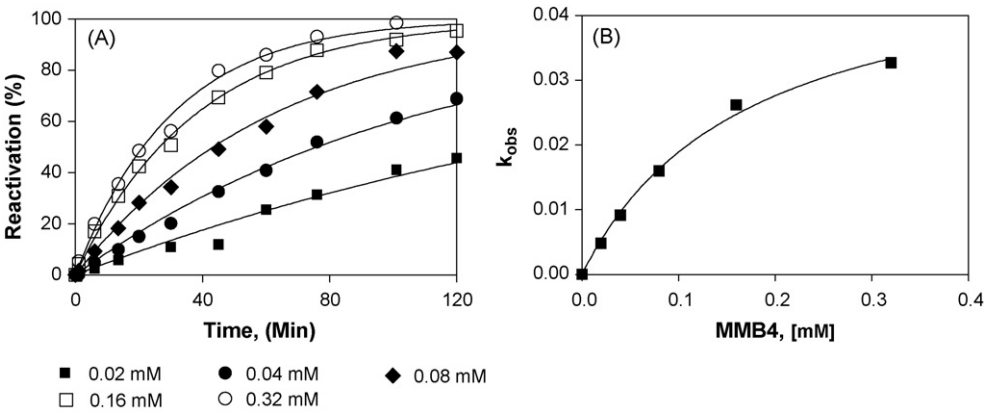

Fig. 3. Reactivation of GF-inhibited wild-type Bo AChE by MMB4. (A) Plot of percent reactivation vs. time to obtain k_{obs} for each concentration of MMB4; (B) plot of k_{obs} vs. [MMB4] to obtain k_r.

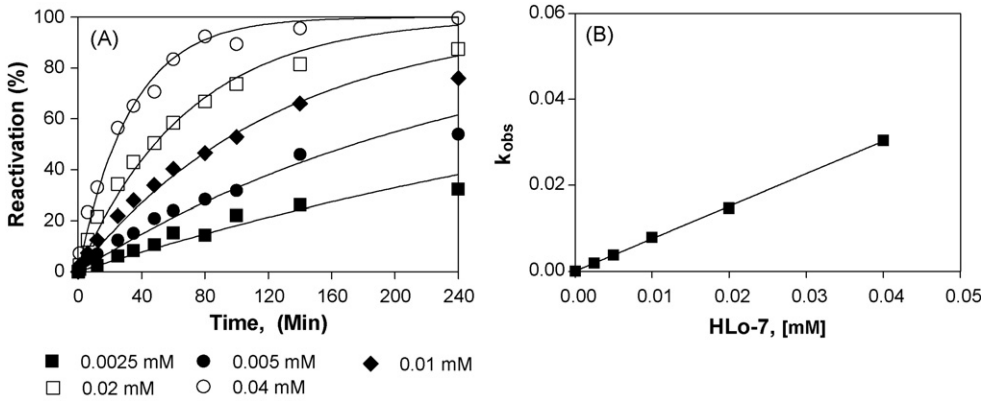

Fig. 4. Reactivation of VR-inhibited Y72N Bo AChE by HLo-7. (A) Plot of percent reactivation vs. time to obtain k_{obs} for each concentration of HLo-7; (B) plot of k_{obs} vs. [HLo-7] to estimate k_r from the slope of the line.

different extents. The mutation of W286 to Ala had the least effect except for reactivation by 2-PAM, which showed a 6-fold reduction (Table 1). The mutation of Y72 to Asn reduced reactivation by bis-pyridinium oximes from 1- to 9-fold, but did not affect reactivation by 2-PAM. The most significant reduction by a single mutation was observed in the reactivation of Y124Q by the two H oximes HI-6 and HLo-7 and HI-6 analog ICD-585 (78-, 43-, and 17-fold, respectively). But, this mutant showed only a 4-fold reduction in reactivation by MMB4 and even promoted reactivation by 2-PAM (Table 1). Interestingly, when Y124 was replaced by Phe, which removed the hydroxyl group while maintaining the aromatic ring, there was very little effect on reactivation by H oximes (Tables 2 and 3). The most dramatic changes observed on oxime reactivation were with a quadruple mutant of the whole PAS residues—Y72N/D74G/Y124Q/W286A. The reactivation of GF-inhibited quadruple mutant Bo AChE by all four bis-pyridinium oximes was 180–1500-fold slower than wild-type AChE. However, only a 3-fold reduction was observed for the reactivation of GF-inhibited quadruple mutant Bo AChE by 2-PAM.

As summarized in Tables 4–6, the overall rate constants for the reactivation of VR-inhibited wild-type Bo AChE by these 5 oximes were relatively similar to that of GF-inhibited AChE. The potency rank order for these oximes was exactly the same as that for GF-

Table 1
Rate constants[a] for the reactivation of GF-inhibited wild-type and mutant Bo AChEs by 2-PAM and MMB4.

Enzyme	2-PAM			MMB4		
	k_2 (min^{-1})	K_{ox} (mM)	k_r ($M^{-1} min^{-1}$)	k_2 (min^{-1})	K_{ox} (mM)	k_r ($M^{-1} min^{-1}$)
Wild-type	0.051 ± 0.017	0.674 ± 0.220	57	0.042 ± 0.024	0.169 ± 0.042	252
Y72N	NA[b]	NA[b]	77	0.005 ± 0.003	0.182 ± 0.093	24
D74G	0.029 ± 0.022	1.920 ± 0.262	15	0.075 ± 0.037	1.041 ± 0.262	410
Y124Q	NA[b]	NA[b]	97	0.102 ± 0.059	2.082 ± 1.410	49
Y124F	0.022 ± 0.004	0.508 ± 0.026	44	0.635 ± 0.246	1.642 ± 0.771	387
W286A	0.026 ± 0.009	3.134 ± 1.102	8	0.106 ± 0.021	0.771 ± 0.127	138
Y337A	0.018 ± 0.008	0.265 ± 0.041	68	0.031 ± 0.015	0.155 ± 0.044	203
Quadruple	NA[b]	NA[b]	13[c]	NA[b]	NA[b]	1.4[c]

[a] Data are mean ± standard errors from 2 to 4 determinations.
[b] Value could not be determined due to the linear relationship of k_{obs} vs. [oxime].
[c] Only one time determination due to the limited availability of this mutant.

Table 2
Rate constants[a] for the reactivation of GF-inhibited wild-type and mutant Bo AChEs by HI-6 and ICD-585.

Enzyme	HI-6			ICD-585		
	k_2 (min^{-1})	K_{ox} (mM)	k_r ($M^{-1} min^{-1}$)	k_2 (min^{-1})	K_{ox} (mM)	k_r ($M^{-1} min^{-1}$)
Wild-type	0.172 ± 0.088	0.126 ± 0.059	1,345	0.128 ± 0.055	0.275 ± 0.129	467
Y72N	NA[b]	NA[b]	482	0.164 ± 0.047	0.472 ± 0.185	347
D74G	0.236 ± 0.083	0.024 ± 0.012	9,990	0.126 ± 0.032	0.053 ± 0.021	2388
Y124Q	0.125 ± 0.027	7.310 ± 1.329	17	0.020 ± 0.015	0.769 ± 0.230	26
Y124F	0.293 ± 0.168	0.552 ± 0.325	531	0.162 ± 0.075	0.602 ± 0.330	269
W286A	NA[b]	NA[b]	471	0.083 ± 0.035	0.173 ± 0.053	478
Y337A	0.311 ± 0.203	0.017 ± 0.013	17,970	NA[b]	NA[b]	8219
Quadruple	NA[b]	NA[b]	1.9[c]	NA[b]	NA[b]	2.0[c]

[a] Data are mean ± standard errors from 2 to 4 determinations.
[b] Value could not be determined due to the linear relationship of k_{obs} vs. [oxime].
[c] Only one time determination due to the limited availability of this mutant.

Table 3
Rate constants[a] for the reactivation of GF-inhibited wild-type and mutant Bo AChEs by HLo-7.

Enzyme	k_2 (min^{-1})	K_{ox} (mM)	k_r ($M^{-1} min^{-1}$)
Wild-type	0.154 ± 0.067	0.045 ± 0.029	3,413
Y72N	0.050 ± 0.021	0.055 ± 0.020	909
D74G	0.401 ± 0.143	0.008 ± 0.002	53,570
Y124Q	0.145 ± 0.066	1.849 ± 0.812	78
Y124F	NA[b]	NA[b]	1,274
W286A	0.098 ± 0.039	0.049 ± 0.028	1,892
Y337A	0.394 ± 0.216	0.075 ± 0.033	52,380
Quadruple	NA[b]	NA[b]	2.3[c]

[a] Data are mean ± standard errors from 2 to 4 determinations.
[b] Value could not be determined due to the linear relationship of k_{obs} vs. [oxime].
[c] Only one time determination due to the availability of this mutant.

inhibited enzyme, indicating the similarity of GF- and VR-inhibited AChE with regard to oxime reactivation. Interestingly, the effects of single and multiple mutations on reactivation by these five oximes were similar too with only a few exceptions. While the overall reactivation rate constants for GF-inhibited D74G AChE by MMB4 and ICD-585 were 0.6- and 4.1-fold higher, that of VR-inhibited AChE was 2.2- and 0.6-fold lower, compared to wild-type AChE. Another difference observed was in reactivation by 2-PAM, with little effect on GF-inhibited conjugate but a 1-fold increase for VR-inhibited enzyme compared with wild-type enzyme. Significant reductions in reactivations of VR-inhibited Y124Q AChE were also observed with HI-6, HLo-7, and ICD-585 (80-, 22-, and 18-fold, respectively), while such reductions were not observed for Y124F AChE. The 580–813-fold reductions in oxime reactivation ability of VR-inhibited quadruple mutant of the PAS by all bis-pyridinium oximes were also observed, but again, only a 3.3-fold reduction was observed with 2-PAM (Tables 4–6).

Molecular modeling studies were conducted to simulate the interaction of 2-PAM and HI-6 before nucleophilic attack on GF- and VR-inhibited Bo AChEs. Since an X-ray crystal structure for Bo AChE was not available and Bo AChE shares 95% sequence homology with human AChE, we built the homology model for Bo AChE using the crystal structure of human AChE. The folds in the homology model of Bo AChE were assumed to be the same as those observed in the crystal structure of human AChE and no differences in the binding sites for the two sequences were observed. Also, a comparison of AChE and BChE structures from different species showed that, the binding site residues are within a root-mean square deviation of 0.5 Å, suggesting that the homology model is good enough for calculations presented in the manuscript.

A plot of the calculated interaction energies of these complexes vs. the experimentally determined K_{ox} values is shown in Fig. 5. Within experimental error, we were able to predict the binding of oximes to GF- and VR-inhibited AChEs with an r^2 value of 0.99. The distances of the nucleophiles from the phosphorus atoms were around 4 Å and the angles of attack were around 150°. Fig. 6A shows the amino acid residues of GF-inhibited Bo AChE that are interacting with 2-PAM. As shown in this figure, the six-membered cyclohexyl group in GF forms a favorable and rigid chair conformation. The critical amino acid residues in the binding site can be grouped into six regions (RI: D74; RII: G82, T83, W86, N87; RIII: S125; RIV: E202; RV: Y337, Y341; and RVI: H447). The calculated interaction energies between 2-PAM and these residues are listed in Table 7, which shows that the major contributions to the binding energies are from two aromatic residues, W86 and Y337. The pyridinium ring of 2-PAM is sandwiched (stacking) between these two aromatic residues: (1) W86 forms a cation-π interaction with the positively charged nitrogen, and (2) the –OH group of Y337 forms an electrostatic interaction with the positively charged nitrogen atom. This "cation-π" stacking helps to position and orient the nucleophile ready for attack on the OP. Fig. 6B shows

Table 4
Rate constants[a] for the reactivation of VR-inhibited wild-type and mutant Bo AChEs by 2-PAM and MMB4.

Enzyme	2-PAM			MMB4		
	k_2 (min^{-1})	K_{ox} (mM)	k_r ($M^{-1} min^{-1}$)	k_2 (min^{-1})	K_{ox} (mM)	k_r ($M^{-1} min^{-1}$)
Wild-type	0.073 ± 0.031	0.938 ± 0.326	79	NA[b]	NA[b]	871
Y72N	NA[b]	NA[b]	78	NA[b]	NA[b]	105
D74G	0.004 ± 0.002	1.729 ± 0.463	2.3	0.042 ± 0.030	0.155 ± 0.079	270
Y124Q	NA[b]	NA[b]	96	NA[b]	NA[b]	181
Y124F	0.078 ± 0.026	0.482 ± 0.215	162	NA[b]	NA[b]	692
W286A	0.027 ± 0.009	0.638 ± 0.212	42	NA[b]	NA[b]	796
Y337A	0.066 ± 0.039	1.082 ± 0.421	61	0.063 ± 0.020	0.081 ± 0.056	780
Quadruple	NA[b]	NA[b]	18[c]	NA[b]	NA[b]	1.5[c]

[a] Data are mean ± standard errors from 2 to 4 determinations.
[b] Value could not be determined due to the linear relationship of k_{obs} vs. [oxime].
[c] Only one time determination due to the limited availability of this mutant.

Table 5
Rate constants[a] for the reactivation of VR-inhibited Bo wild-type and mutant AChEs by HI-6 and ICD-585.

Enzyme	HI-6			ICD-585		
	k_2 (min^{-1})	K_{ox} (mM)	k_r ($M^{-1}\,min^{-1}$)	k_2 (min^{-1})	K_{ox} (mM)	k_r ($M^{-1}\,min^{-1}$)
Wild-type	0.207 ± 0.110	0.094 ± 0.047	2193	0.167 ± 0.092	0.188 ± 0.010	896
Y72N	NA[b]	NA[b]	419	NA[b]	NA[b]	297
D74G	0.456 ± 0.144	0.051 ± 0.019	9038	0.201 ± 0.064	0.369 ± 0.089	543
Y124Q	0.053 ± 0.039	0.1.963 ± 1.426	27	0.041 ± 0.022	0.841 ± 0.332	48
Y124F	0.172 ± 0.079	0.830 ± 0.311	823	0.093 ± 0.018	0.324 ± 0.052	287
W286A	NA[b]	NA[b]	1052	0.099 ± 0.025	0.098 ± 0.051	1017
Y337A	0.054 ± 0.031	0.007 ± 0.005	8072	0.213 ± 0.136	0.049 ± 0.033	4380
Quadruple	NA[b]	NA[b]	3.7[c]	NA[b]	NA[b]	4.5[c]

[a] Data are mean ± standard errors from 2 to 4 determinations.
[b] Value could not be determined due to the linear relationship of k_{obs} vs. [oxime].
[c] Only one time determination due to the limited availability of this mutant.

the amino acid residues of VR-inhibited Bo AChE that are interacting with 2-PAM. The conclusions from this model are similar to those from the GF-inhibited Bo AChE·2-PAM complex except the iso-butyl group in VR is flexible enough to move and fill up the binding pocket better than the rigid cyclohexyl ring in GF. The calculated interaction energies between 2-PAM and the critical residues listed in Table 7 are also similar. The mutation of Y337 to Ala will provide additional space for the accommodation of 2-PAM, which will result in increased reactivation, as was observed in reactivation studies with the Y337A mutant. In both models, the R-groups of GF and VR point toward the pockets formed by four amino acid regions: RI: F123, Y124; RII: W236; RIII: F295, F297, V300; and RIV: W407. This binding pocket can accommodate R-groups of various sizes—small as in GB as well as larger groups as in GD, GF and VR. Amino acid residues Y72, D74, and W286 at the PAS do not interact with 2-PAM and thereby do not affect the reactivation abilities of 2-PAM.

Fig. 7A shows the amino acid residues of GF-inhibited Bo AChE that are interacting with HI-6. In this case, critical amino acid residues in the binding site can be grouped into seven regions (RI: Y72, D74; RII: G82, T83, D84, W86, N87; RIII: Y124, S125; RIV: E202; RV: Y337, Y341; RVI: H447; and RVII: W286, R287). The calculated interaction energies between HI-6 and these residues are listed in Table 7, which shows that the major contributions to the binding energies are from three residues, D74, W86 and Y337. The binding sites of the pyridinium rings containing the oxime are the same as those for the 2-PAM models. However, the "sandwich" stacking energies between the pyridinium ring containing the oxime and W86 and Y337 are more favored with HI-6 because of interactions with the oxygen in the linker connecting the two pyridinium rings. The negatively charged carboxyl group of D74 interacts favorably via electrostatic interactions with the positively charged nitrogen in the two pyridinium rings of HI-6. Y124 interacts favorably with HI-6 via an end-on stacking with the pyridinium ring containing the amide group. As indicated above, additional van der Waals and electrostatic interactions for HI-6 were identified with W286 and R287, respectively, in the seventh region (RVII), but the net interaction energy is −0.2 kcal. This suggests that HI-6 makes a weak contact with W286. Fig. 7B shows the amino acid residues of VR-inhibited Bo AChE that are interacting with HI-6. The conclusions from this model are similar to those from the GF-inhibited Bo AChE·HI-6 complex. The calculated interaction energies between HI-6 and amino acid residues suggest that the binding of HI-6 is favored with VR-inhibited Bo AChE compared to GF-inhibited Bo AChE.

Table 6
Rate constants[a] for the reactivation of VR-inhibited wild-type and mutant Bo AChEs by HLo-7.

Enzyme	k_2 (min^{-1})	K_{ox} (mM)	k_r ($M^{-1}\,min^{-1}$)
Wild-type	0.373 ± 0.224	0.096 ± 0.062	3,892
Y72N	NA[b]	NA[b]	1,080
D74G	NA[b]	NA[b]	10,835
Y124Q	0.307 ± 0.131	1.807 ± 1.229	170
Y124F	0.169 ± 0.051	0.084 ± 0.026	2,017
W286A	NA[b]	NA[b]	1,648
Y337A	0.401 ± 0.286	0.055 ± 0.026	7,309
Quadruple	NA[b]	NA[b]	5.4[c]

[a] Data are mean ± standard errors from 2 to 4 determinations.
[b] Value could not be determined due to the linear relationship of k_{obs} vs. [oxime].
[c] Only one time determination due to the availability of this mutant.

4. Discussion

Oxime reactivation of nerve agent-inhibited AChE proceeds via nucleophilic attack on the phosphorus atom and is greatly facilitated by the proper orientation of the nucleophile in the active-site of the enzyme. The facilitation for mono-pyridinium oxime 2-PAM is due to the interaction of the positively charged pyridinium ring with residues in the CAS of the enzyme. Bis-pyridinium oximes, on the other hand, may use the second-pyridinium ring to interact with residues at the PAS to facilitate reactivation. Indeed, results from this study using wild-type and different mutant Bo AChEs indicate that when all four PAS residues were replaced, reactivation rates were reduced from 180- to 1500-fold. This explains the superiority of bis-pyridinium oximes over the mono-pyridinium oxime, especially when the enzyme is inhibited by nerve agents with bulky side-chains such as soman, GF, and VR. In fact, reactivation rate constants for GF- and VR-inhibited quadruple mutant by all four bis-pyridinium oximes

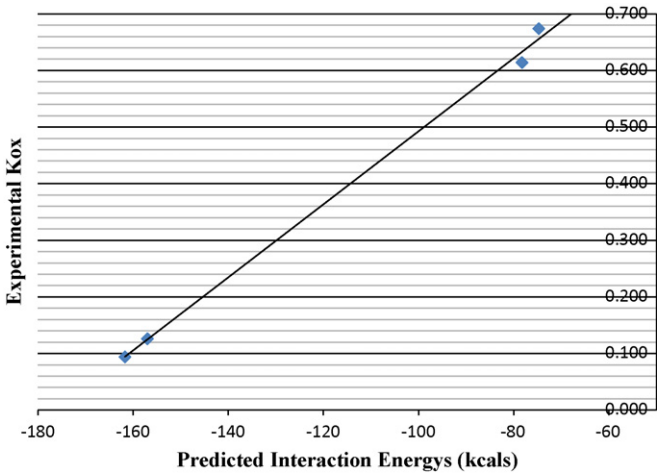

Fig. 5. A plot of experimentally determined binding constants vs. calculated interaction energies for various oximes.

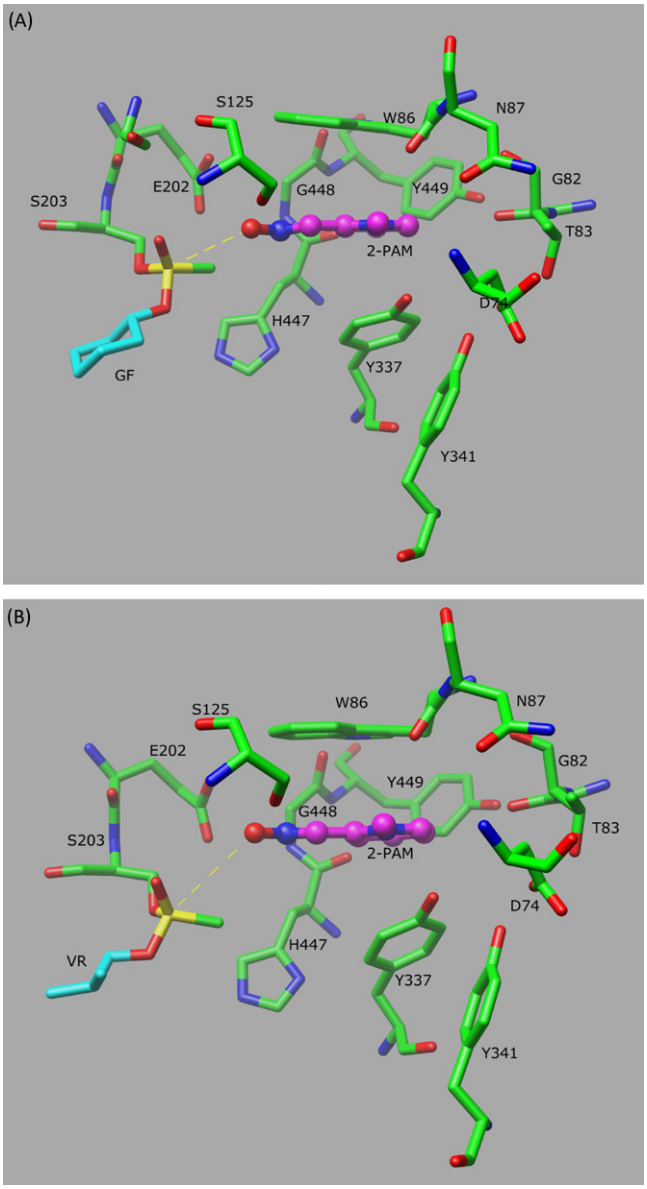

Fig. 6. The binding site of 2-PAM in the energy minimized models of GF-inhibited Bo AChE (A) and VR-inhibited Bo AChE (B). Amino acid residues with binding energies equal to or less than −1.0 kcal with 2-PAM are shown and labeled. Amino acid residues of Bo AChE are shown as color-coded bonds based on atoms (carbon: green, oxygen: red, nitrogen: blue, phosphorus: yellow). The color coding for 2-PAM is the same except that carbon: magenta. Nucleophilic attack on OP is shown by yellow dashed lines. The cyclohexyl group of GF and the iso-butyl group of VR are shown in cyan in panels A and B, respectively. Hydrogen atoms are not shown for clarity.

were several fold lower than that for the mono-pyridinium oxime 2-PAM even though they were over 50 times more potent (such as HLo-7) before the PAS residues were mutated. The data provide very strong evidence that these bis-pyridinium oximes reactivate nerve agent-inhibited AChE by interacting with residues at the PAS of the enzyme. It also indicates that the larger bis-pyridinium oximes are less flexible than the mono-pyridinium oxime in interacting with residues at the CAS, since three of the four bis-pyridinium oximes (HI-6, HLo-7, and ICD-585), which contain a first pyridinium ring that is identical to 2-PAM, demonstrated lower reactivation ability when these PAS residues were replaced. A previous study with recombinant mouse AChE inhibited by MEPQ, demonstrated that triple mutation (W286A/Y72N/Y124Q)

Table 7
Calculated interaction energies (in kcal) between the oxime and the critical amino acid residues in GF- and VR-inhibited Bo AChEs.

Amino acids	GF-2-PAM	VR-2-PAM	GF-HI-6	VR-HI-6
RI				
Y72	–	–	−7.3	−7.6
D74	−5.5	−4.9	−37.7	−38.1
RII				
G82	−7.8	−7.6	−8.5	−9.2
T83	−4.2	−4.1	−6.3	−6.7
D84	–	–	−3.5	−3.7
W86	−14.7	−14.2	−26.0	−24.9
N87	−3.7	−3.4	−10.8	−11.0
RIII				
Y124	–	–	−3.9	−5.5
S125	−2.0	−2.3	−4.4	−3.7
RIV				
E202	−2.4	−3.1	−4.8	−4.7
RV				
Y337	−12.8	−12.7	−16.8	−17.0
Y341	−2.0	−2.0	−6.0	−6.1
RVI				
H447	−4.4	−5.0	−4.3	−3.8
RVII				
W286	–	–	0.9	−0.8
R287	–	–	−1.1	−1.1

at the PAS significantly decreased the reactivation ability of HI-6 but to a lesser extent by 2-PAM possibly due to the less bulky OP structure of MEPQ compared to that of GF and VR [26]. Therefore, our results suggest that the second-pyridinium structure plays a crucial role in the enhanced reactivation activity of all bis-pyridinium oximes over the mono-pyridinium oxime.

Results of single amino acid substitutions at the PAS revealed that most single residue changes affected oxime reactivation moderately. Of all the four bis-pyridinium oximes tested, the most significant reductions were observed with Y124 Q AChE when HI-6, HLo-7, and ICD-585 were used as reactivators. However, when Y124 was replaced with Phe, there was no significant drop in the reactivation ability of these oximes, indicating that the facilitation effect of Tyr is through interaction with the aromatic structure, and not through the hydroxyl group. Indeed, results of modeling studies support such a stacking interaction of the second-pyridinium ring with Y124 for both GF- and VR-inhibited Bo AChE (Fig. 7A and B). In the active-site of AChE, F297, Y124, W286 and Y72 form a cluster of aromatic amino acids with favorable stacking interactions. F297 interacts with the R-group of OP nerve agent, while W286 and Y72 form stacking interactions. Y124 is critical in maintaining the binding pocket for interactions with the second-pyridinium ring of H oximes and also forms favorable end-on stacking interactions with F297 and W286. This is only possible if the residue at position 124 is either Tyr or Phe and any change in these interactions will be relayed like a "domino effect" to the peripheral residues W286 and Y72.

Previously, the X-ray crystal structure of mouse AChE·HI-6 complex revealed that the second-pyridinium ring of HI-6 could form a sandwich stacking with Y124 and W286 [29]. This interaction was also observed in the X-ray structure of a co-crystal of HI-6 with GB-inhibited mouse AChE [37]. The involvement of W286 in such a sandwich interaction in GF- and VR-inhibited Bo AChE·HI-6 complex is not supported by our site-directed mutagenesis studies since the mutation of W286 to Ala reduced the reactivation abilities of H oximes by a maximum of 2-fold. The results of modeling studies with both GF- and VR-inhibited Bo AChE·HI-6 complexes did not show the involvement

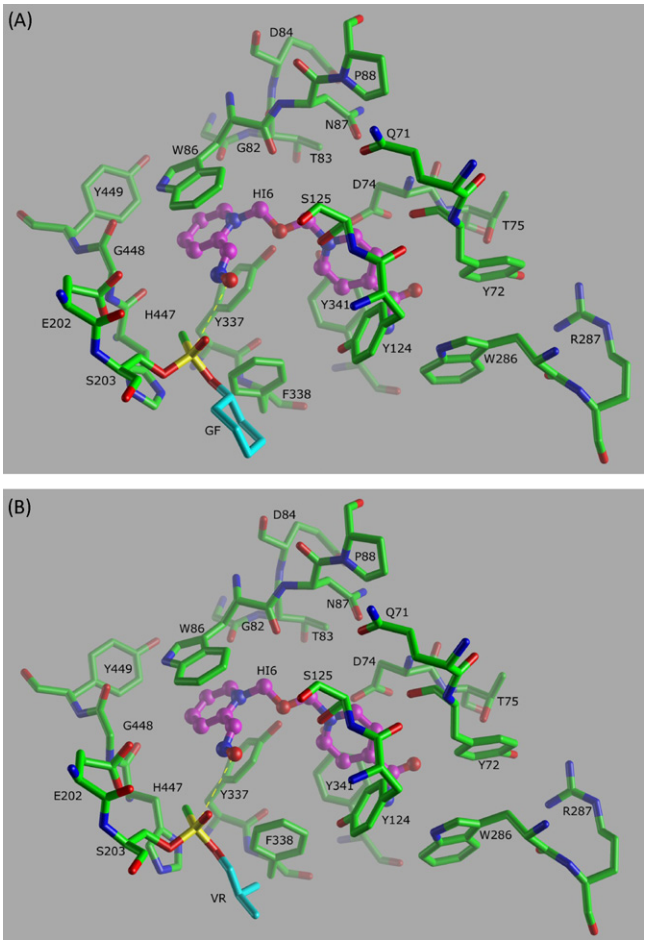

Fig. 7. The binding site of HI-6 in the energy minimized models of GF-inhibited Bo AChE (A) and VR-inhibited Bo AChE (B). Amino acid residues with binding energies equal to or less than −1.0 kcal with HI-6 are shown and labeled. Amino acid residues of Bo AChE are shown as color-coded bonds based on atoms (carbon: green, oxygen: red, nitrogen: blue, phosphorus: yellow). The color coding for HI-6 is the same except that carbon: magenta. Nucleophilic attack on OP is shown by yellow dashed lines. The cyclohexyl group of GF and the iso-butyl group of VR are shown in cyan in panels A and B, respectively. Hydrogen atoms are not shown for clarity (For interpretation of the references to color in this figure legend, the reader is referred to the web version of the article.).

of W286 in a sandwich stacking either. These results suggest that the position and interaction of HI-6 with residues at the PAS of AChE is not only influenced by the presence of OP in the active-site of AChE, but also by the structure of OP compound.

The loss of a negative charge as in D74G AChE is expected to weaken the interaction with the positively charged oxime. As shown in Table 7, the negatively charged side-chain of D74 interacts very strongly with the two positive charges of H oximes compared to any other interactions. The charge–charge interactions might affect the release of the products. Thus, the mutation of D74 to Gly will reduce this interaction and enhance the reactivation process. Although, the energy for the interaction of D74 with 2-PAM (Table 7) is less compared to that for its interaction with HI-6, but the significance of this interaction is demonstrated by the reduced reactivation of the D74G mutant by 2-PAM. The active-site mutant Y337A AChE also showed increased oxime reactivation in most cases. Results of modeling studies suggest that the removal of aromatic residue at the active center of the enzyme may enlarge the available space for bis-pyridinium oximes and therefore facilitate oxime reactivation, which was also observed with mouse AChE [17].

In summary, the results of this study on oxime reactivation of wild-type and mutant Bo AChEs reveal that amino acid residues at the PAS as a whole group play a critical role in the enhanced reactivation ability of all bis-pyridinium oximes compared to mono-pyridinium oxime. Y124 is an important residue for the potent reactivation ability of HI-6, ICD-585, and HLo-7, but has much less or no involvement in reactivation by MMB4 and 2-PAM. A comparison of the reactivation of nerve agent-inhibited Y124Q and Y124F AChEs by these bis-pyridinium oximes and molecular modeling studies did not support the sandwich interaction of Y124, W286 and the second-pyridinium structure of HI-6 proposed by X-ray crystallographic studies of HI-6·AChE and GB-inhibited AChE·HI-6 complexes. Instead, the data are more supportive to the stacking between H oximes and Y124 only. Although these results were obtained with GF and VR, two nerve agents containing bulky side-chains, the enhanced reactivation of soman-inhibited AChE by H oximes has been demonstrated in many previous studies [3,9,24]. The reported molecular volume of GF's OR group is about 25–30% more than that for VR [38,39]. The calculated molecular volume for the six-carbon pinacolyl group of soman is only 9% more than that for the cyclohexyl group of GF (unpublished observation). Unfortunately, the fast aging of soman-inhibited enzyme precludes the accurate determination of reactivation rate constants, thus it is difficult to compare the reactivation potency of H oximes toward soman- and GF-inhibited AChEs. However, results of this study highlight the contribution of the interaction between Tyr124 and the amide-containing pyridinium ring of H oximes for their potency in reactivating AChE inhibited by bulky side-chain nerve agents.

Conflict of interest

The authors declare that there are no conflicts of interest.

Acknowledgements

We thank Mr. Patrick Kates and Mr. Shawn Xiao for the excellent technical assistance and Dr. Robert diTargiani providing purified rabbit PON1. This work was supported by funding from the Defense Threat Reduction Agency. The opinions or assertions contained herein are the private views of the authors and are not to be construed as official or as reflecting the views of the US Army or the Department of Defense.

References

[1] Marrs TC. Clinical and experimental toxicology of organophosphates and carbamates. Oxford: Butterworth & Heinemann; 1992. p. 555–77.
[2] Puu G, Artursson E, Bucht G. Reactivation of nerve agent inhibited human acetylcholinesterases by HI-6 and obidoxime. Biochem Pharmacol 1986;35:1505–10.
[3] Worek F, Thiermann H, Szinicz L, Eyer P. Kinetic analysis of interactions between human acetylcholinesterase, structurally different organophosphorus compounds and oximes. Biochem Pharmacol 2004;68:2237–48.
[4] Sidell FR. Textbook of military medicine: medical aspects of chemical and biological warfare (Bordon Institute ed.); 1997. p. 129–36.
[5] Oldiges H, Schoene K. Pyridinium and imidazolium salts as antidotes for soman and paraoxon poisoning in mice. Arch Toxicol 1970;26:293–305.
[6] de Jong LP, Wolring GZ. Reactivation of acetylcholinesterase inhibited by 1,2,2′-trimethylpropyl methylphosphonofluoridate (soman) with HI-6 and related oximes. Biochem Pharmacol 1980;29:2379–87.
[7] Lundy PM, Hansen AS, Hand BT, Boulet CA. Comparison of several oximes against poisoning by soman, tabun and GF. Toxicology 1992;72:99–105.
[8] Boskovic B, Kovacevic V, Jovanovic D. PAM-2 Cl, HI-6, and HGG-12 in soman and tabun poisoning. Fundam Appl Toxicol 1984;4:S106–15.
[9] de Jong LP, Verhagen MA, Langenberg JP, Hagedorn I, Loffler M. The bispyridinium-dioxime HLo-7. A potent reactivator for acetylcholinesterase inhibited by the stereoisomers of tabun and soman. Biochem Pharmacol 1989;38:633–40.
[10] Eyer P, Ladstetter B, Schafer W, Sonnenbichler J. Studies on the stability and decomposition of the Hagedorn-oxime HLo 7 in aqueous solution. Arch Toxicol 1989;63:59–67.

[11] Ashani Y, Cohen S. Nucleophilicity of some reactivators of phosphorylated acetylcholinesterase. J Med Chem 1971;14:621–6.
[12] Su CT, Tang CP, Ma C, Shih YS, Liu CY, Wu MT. Quantitative structure–activity relationships and possible mechanisms of action of bispyridinium oximes as antidotes against pinacolyl methylphosphonofluoridate. Fundam Appl Toxicol 1983;3:271–7.
[13] Wong L, Radic Z, Bruggemann RJM, Hosea N, Berman HA, Taylor P. Mechanism of oxime reactivation of acetylcholinesterase analyzed by chirality and mutagenesis. Biochemistry 2000;39:5750–7.
[14] Kovarik Z, Radic Z, Berman HA, Simeon-Rudolf V, Reiner E, Taylor P. Mutant cholinesterases possessing enhanced capacity for reactivation of their phosphonylated conjugates. Biochemistry 2004;43:3222–9.
[15] Sussman JL, Harel M, Frolow F, Oefner C, Goldman A, Toker L, et al. Atomic structure of acetylcholinesterase from Torpedo californica: a prototypic acetylcholine-binding protein. Science 1991;253:872–9.
[16] Johnson JL, Thomas JL, Emani S, Cusack B, Rosenberry TL. Measuring carbamoylation and decarbamoylation rate constants by continuous assay of AChE. Chem Biol Interact 2005;157–158:384–5.
[17] Colletier JP, Fournier D, Greenblatt HM, Stojan J, Sussman JL, Zaccai G, et al. Structural insights into substrate traffic and inhibition in acetylcholinesterase. EMBO J 2006;25:2746–56.
[18] Harvey B, Scott RP, Sellers DJ, Watts P. In vitro studies on the reactivation by oximes of phosphylated acetylcholinesterase—II. On the formation of O,O-diethyl phosphorylated AChE and O-ethyl methylphosphonylated AChE and their reactivation by PS2. Biochem Pharmacol 1986;35:745–51.
[19] de Jong LP, Wolring GZ. Stereospecific reactivation by some Hagedorn-oximes of acetylcholinesterases from various species including man, inhibited by soman. Biochem Pharmacol 1984;33:1119–25.
[20] Talbot BG, Anderson DR, Harris LW, Yarbrough LW, Lennox WJ. A comparison of in vivo and in vitro rates of aging of soman-inhibited erythrocyte acetylcholinesterase in different animal species. Drug Chem Toxicol 1988;11:289–305.
[21] Worek F, Eyer P, Szinicz L. Inhibition, reactivation and aging kinetics of cyclohexylmethylphosphonofluoridate-inhibited human cholinesterases. Arch Toxicol 1998;72:580–7.
[22] Clement JG. Efficacy of various oximes against GF (cyclohexyl methylphosphonofluoridate) poisoning in mice. Arch Toxicol 1992;66:143–4.
[23] Luo C, Liang J. Evaluation of combined toxic effects of GB/GF and efficacy of jielin injection against combined poisoning in mice. Toxicol Lett 1997;92:195–200.
[24] Luo CY, Tong M, Chilukuri N, Brecht K, Maxwell DM, Saxena A. An in vitro comparative study on the reactivation of nerve agent-inhibited guinea pig and human acetylcholinesterases by oximes. Biochemistry 2007;46:11771–9.
[25] Maxwell DM, Koplovitz I, Worek F, Sweeney RE. A structure–activity analysis of the variation in oxime efficacy against nerve agents. Toxicol Appl Pharmacol 2008;231:157–64.
[26] Ashani Y, Radic Z, Tsigelny I, Vellom DC, Pickering NA, Quinn DM, et al. Amino acid residues controlling reactivation of organophosphonyl conjugates of acetylcholinesterase by mono- and bisquaternary oximes. J Biol Chem 1995;270:6370–80.
[27] Hammond PI, Kern C, Hong F, Kollmeyer TM, Pang YP, Brimijoin S. Cholinesterase reactivation in vivo with a novel bis-oxime optimized by computer-aided design. J Pharmacol Exp Ther 2003;307:190–6.
[28] Ekstrom F, Pang YP, Boman M, Artursson E, Akfur C, Borjegren S. Crystal structures of acetylcholinesterase in complex with HI-6, Ortho-7 and obidoxime: structural basis for differences in the ability to reactivate tabun conjugates. Biochem Pharmacol 2006;72:597–607.
[29] Ekstrom FJ, Astot C, Pang YP. Novel nerve-agent antidote design based on crystallographic and mass spectrometric analyses of tabun-conjugated acetylcholinesterase in complex with antidotes. Clin Pharmacol Ther 2007;82:282–93.
[30] Ellman GL, Courtney KD, Andres Jr V, Feather-Stone RM. A new and rapid colorimetric determination of acetylcholinesterase activity. Biochem Pharmacol 1961;7:88–95.
[31] Luo CY, Saxena A, Smith M, Garcia G, Radic Z, Taylor P, et al. Phosphoryl oxime inhibition of acetylcholinesterase during grime reactivation is prevented by edrophonium. Biochemistry 1999;38:9937–47.
[32] Stenzel J, Worek F, Eyer P. Preparation and characterization of dialkylphosphoryl-obidoxime conjugates, potent anticholinesterase derivatives that are quickly hydrolyzed by human paraoxonase (PON1192Q). Biochem Pharmacol 2007;74:1390–400.
[33] Gan KN, Smolen A, Eckerson HW, La Du BN. Purification of human serum paraoxonase/arylesterase. Evidence for one esterase catalyzing both activities. Drug Metab Dispos 1991;19:100–6.
[34] Doctor BP, Chapman TC, Christner CE, Deal CD, De La Hoz DM, Gentry MK, et al. Complete amino acid sequence of fetal bovine serum acetylcholinesterase and its comparison in various regions with other cholinesterases. FEBS Lett 1990;266:123–7.
[35] Kryger G, Harel M, Giles K, Toker L, Velan B, Lazar A, et al. Structures of recombinant native and E202Q mutant human acetylcholinesterase complexed with the snake-venom toxin fasciculin-II. Acta Crystallogr D Biol Crystallogr 2000;56:1385–94.
[36] Kryger G, Giles K, Harel M, Toker L, Velan B, Lazar A, et al. 3D structure of a complex of human acetylcholinesterase with fasciculin-II at 2.7 angstrom resolution. In: Doctor BP, Quinn DM, Rotundo RL, Taylor P, editors. Structure and function of cholinesterases and related proteins. New York: Plenum Publishing Corporation; 1998. p. 370.
[37] Ekstrom F, Hornberg A, Artursson E, Hammarstrom LG, Schneider G, Pang YP. Structure of HI-6*sarin-acetylcholinesterase determined by X-ray crystallography and molecular dynamics simulation: reactivator mechanism and design. PLoS One 2009;4:e5957.
[38] Maxwell D, Koplovitz I, Worek F, Sweeney RE. A structure–activity analysis of the variation in oxime efficacy against nerve agents. Toxicol Appl Pharmacol 2008;231:157–64.
[39] Luo C, Chambers C, Yang Y, Saxena A. Mechanism for potent reactivation ability of H oximes analyzed by reactivation kinetic studies with cholinesterases from different species. Chem Biol Interact 2010. E-pub ahead of press.